

Non-Wigner-Dyson level statistics and fractal wavefunction of disordered Weyl semimetals

C. Wang^{1,2}, Peng Yan¹, and X. R. Wang^{2,3*}

¹*School of Electronic Science and Engineering and State Key Laboratory of Electronic Thin Film and Integrated Devices, University of Electronic Science and Technology of China, Chengdu 610054, China*

²*Physics Department, The Hong Kong University of Science and Technology, Clear Water Bay, Kowloon, Hong Kong and*

³*HKUST Shenzhen Research Institute, Shenzhen 518057, China*

(Dated: March 14, 2022)

Finding fingerprints of disordered Weyl semimetals (WSMs) is an unsolved task. Here we report such findings in the level statistics and the fractal nature of electron wavefunction around Weyl nodes of disordered WSMs. The nearest-neighbor level spacing follows a new universal distribution $P_c(s) = C_1 s^2 \exp[-C_2 s^{2-\gamma_0}]$ originally proposed for the level statistics of critical states in the integer quantum Hall systems or normal dirty metals (diffusive metals) at metal-to-insulator transitions, instead of the Wigner-Dyson distribution for diffusive metals. Numerically, we find $\gamma_0 = 0.62 \pm 0.07$. In contrast to the Bloch wavefunctions of clean WSMs that uniformly distribute over the whole space of ($D = 3$) at large length scale, the wavefunction of disordered WSMs at a Weyl node occupies a fractal space of dimension $D = 2.18 \pm 0.05$. The finite size scaling of the inverse participation ratio suggests that the correlation length of wavefunctions at Weyl nodes ($E = 0$) diverges as $\xi \propto |E|^{-\nu}$ with $\nu = 0.89 \pm 0.05$. In the ergodic limit, the level number variance Σ_2 around Weyl nodes increases linearly with the average level number N , $\Sigma_2 = \chi N$, where $\chi = 0.2 \pm 0.1$ is independent of system sizes and disorder strengths.

Crystal Weyl semimetals (WSMs), characterized by the linear crossings of their conduction and valence bands at Weyl nodes (WNs) and topologically protected surface states, have attracted enormous attention in recent years because of their exotic properties and potentials in applications [1–8]. There is little doubt that WSMs are a new state of matter in nature. However, the characteristics of WSMs for a crystal do not apply to a disordered system since the lattice momentum is not a good quantum number. To fully establish the WSMs as a genuine state of matter, one needs to find their fingerprints in disorders that inevitably exist in all materials. It was originally believed that disordered WSMs are featured by vanishing density of states (DOS) at WNAs [9–13]. The divergence of the bulk state localization length at the Weyl-semimetal-to-diffusive-metal (WSM-to-DM) transition was also conjectured [14–18]. Nonetheless, these features were challenged in many recent studies [19–22]. So far, a simple working criterion for disordered WSMs is still lacking. This study aims to search the fingerprints from the random matrices that describe the disordered WSMs.

Random matrices have broad applications in many fields of physics [23–27]. In the condensed matter physics, random matrix theory can be used to distinguish different types of metals. The distribution $P(s)$ of nearest-neighbour level spacing s (in the unit of the mean level spacing) of diffusive metals (normal dirty metals) and the level number variance $\Sigma_2(\Delta E) = \langle n^2 \rangle - \langle n \rangle^2$ in a given energy range are governed by the Wigner-Dyson distributions [28]. For example, $P(s)$ follows the Wigner surmises, $P_\beta(s) = C_1 s^\beta \exp[-C_2 s^2]$ (C_1 and C_2 are determined by the probability normalization and the unity of mean level spacing $\int P_\beta(s) ds = \int s P_\beta(s) ds = 1$), where $\beta = 1, 2$ and 4 , depending on symmetries [29]. They are in contrast to the Poisson distribution $P_{\text{Loc}}(s) = \exp[-s]$ for level spacings of Anderson insulators. One interesting and fundamental question is whether level statistics can be used to distinguish disordered WSMs from normal dirty metals.

Far from the WNAs, the level statistics of extended states of a

disordered WSM should not behave differently from those of diffusive metals (DMs). However, near the WNAs, the numbers of extended states are few [30]. In another word, extended states tend to avoid these points besides their general level repulsion effect. Thus, this “double” repulsion should result in weak decay of $P(s)$ in the tail. On this aspect, WNAs are very similar to the critical points located near each Landau subband [31, 32] of the integer quantum Hall (IQH) systems where there is only one extended state, or the conventional metal-insulator transition point where the density of extended states is also vanishingly small. The level statistics of the extended states in IQH systems and near a metal-insulator transition point are believed to follow a new *critical* level statistics $P_c(s)$ [33–39]. For Gaussian unitary ensemble (GUE) [29], a sub-Gaussian decay of $P_c(s)$ and a linear increase of $\Sigma_2(\Delta E)$ with the mean level number N were predicted:

$$P_c(s) = C_1 s^2 \exp[-C_2 s^{2-\gamma_0}], \quad (1)$$

and

$$\Sigma_2(\Delta E) = \chi N, \quad (2)$$

that differ from the Wigner-Dyson distributions mentioned early. Here $\gamma_0 = 1 - 1/(vd)$ with the correlation length critical exponent ν and the spatial dimension d . $\chi > 0$ is a universal constant, known as the “spectral compressibility”. Naturally, one suspects that extended states in the vicinity of the WNAs follow the critical level statistics. The focus of the current work is to see whether this conjecture is correct or not, and whether it can be a fingerprint of disordered WSMs.

In this work, we use the exact diagonalization method to compute the eigenenergies and eigenfunctions of a disordered WSM on a cubic lattice. Through the finite-size scaling analysis of the inverse participation ratio (IPR), we find that the wavefunctions at WNAs ($E = 0$) are fractals of dimension 2.18 ± 0.05 . The finite size scaling of the IPR reveals the correlation length $\xi(E)$ of wavefunctions around WNAs diverging as $\xi = \xi_0(W)|E/t|^{-\nu} a$ with $\nu = 0.89 \pm 0.05$, where a and

t are respectively the lattice constant and the hopping energy. $\xi_0(W)$ is a disorder-dependent dimensionless coefficient. For a finite system of size L , the energy level spacing distribution $P(s)$ within the energy window of $|E| < \epsilon_c = t(\xi_0 a/L)^{1/\nu}$ follows the critical distribution $P_c(s)$, while the level spacing of extended states outside the energy window is described by the Wigner-Dyson distribution $P_{\beta=2}(s)$. For a small energy range ΔE within which the average level number N is small, the level number variance $\Sigma_2(\Delta E)$ around WNs is linear in N , $\Sigma_2(\Delta E) = \chi N$, with a disorder-independent constant $\chi = 0.2 \pm 0.1$. At moderate disorders where the pair of WNs annihilate each other, $\Sigma_2(\Delta E)$ increases logarithmically with N , in agreement with the Wigner-Dyson prediction for GUE.

Model and methods.—To substantiate our claims, we consider a tight-binding Hamiltonian on a cubic lattice of size L^3 and unity lattice constant $a = 1$,

$$H = H_0 + V. \quad (3)$$

The first term is for a pure system,

$$H_0 = \sum_i m_z c_i^\dagger \sigma_z c_i - \sum_i \left[\frac{m_0}{2} (c_{i+\hat{x}}^\dagger \sigma_z c_i + c_{i+\hat{y}}^\dagger \sigma_z c_i) + \frac{t}{2} (c_{i+\hat{z}}^\dagger \sigma_z c_i + ic_{i+\hat{x}}^\dagger \sigma_x c_i + ic_{i+\hat{y}}^\dagger \sigma_y c_i + H.c.) \right], \quad (4)$$

where $c_i^\dagger = (c_{i\uparrow}^\dagger, c_{i\downarrow}^\dagger)$ and c_i are the single electron creation and annihilation operators at site i . $\hat{x}, \hat{y}, \hat{z}$ are the unit lattice vectors along the x, y, z directions, respectively. $\sigma_{x,y,z}$ are the Pauli matrices for spin. m_z and m_0 are respectively Dirac and Newtonian masses. Hereafter we take $m_0/t = 2.1$ and $m_z/t = 0$ with t being the energy unit such that H_0 is a WSM with two pairs of WNs at $E = 0$ [16]. Disorders are introduced through the second term

$$V = \sum_i V_i^0 \sigma_0 + V_i^z \sigma_z, \quad (5)$$

where V_i^0 and V_i^z distribute randomly and uniformly in the range of $[-W/2, W/2]$ such that W measures the randomness strength. Of course, one could also introduce the disorders by other terms such as $V = \sum_i V_i^x \sigma_x + V_i^y \sigma_y$, but the physics does not change [40].

Hamiltonians (4) and (5) were used in Refs. [13, 15–17, 21] to study phase transitions from disordered WSMs to various other quantum phases. Disordered WSMs in this model break the time-reversal symmetry and belong to the GUE with symmetric index $\beta = 2$ [29]. Early numerical calculations [16, 18, 21] of localization lengths and averaged Hall conductivities have established following results for the model when the Fermi level is at $E = 0$: 1) In the weak disorder of $W \leq W_{c,1} \simeq 5.2$, the system is a disordered WSM. 2) For the intermediate disorder of $W_{c,3} \simeq 21 > W > W_{c,2} \simeq 6.2$, the system is a normal (without topological surface states) DM. 3) For strong disorder of $W > W_{c,3}$, the state of $E = 0$ is localized, and the system is an Anderson insulator. Whether there is a phase transition between $W_{c,1}$ and $W_{c,2}$ is an issue under

debate [21]. Later, we shall provide convincing evidence in the level statistics that this is a direct WSM-to-DM transition.

We use the exact diagonalization method to obtain all eigenenergies and eigenfunctions. The IPR, defined as $p_2(E) = \langle \sum_i |\psi_i(E)|^4 \rangle^{-1}$ where $\psi_i(E)$ is the amplitude of normalized wavefunction of energy E at site i , is used to study the wavefunction structure. IPR measures the number of sites that the state occupies and scales with sizes as $p_2 \sim \text{const} [p_2 \propto L^d]$ for a localized (normal extended) state [42]. If there exists an isolated critical state at E_c whose wavefunction is a fractal, the one-parameter scaling analysis says that IPR of the states near E_c is a universal function of the fractal dimension D ($0 < D < d$) [11, 42, 43],

$$p_2(E) = L^D [f(L/\xi) + C_3/L^y], \quad (6)$$

where $f(x)$ is an unknown scaling function, C_3 is the coefficient of the finite-size correction, and $y > 0$ is the exponent for the irrelevant variable. The correlation length ξ diverges as $\xi = \xi_0 |E - E_c|^{-\nu}$, where ν is the critical exponent characterizing the universality class. The state wavefunction occupies a fractal (whole) space of dimensionality $D \neq 3$ ($d = 3$) if the system size is smaller (larger) than ξ .

In our analysis, we fit the numerically obtained $p_2(E)$ by Eq. (6) [40]. The identification of whether a state is extended, localized, or critical is guided by the following criteria: (1) For extended (localized) states, $Y_L(E) = p_2 L^{-D} - C_3/L^y$ increases (decreases) with system size L ; (2) For critical states, $Y_L(E) = f(L/\xi)$ is the one-parameter scaling function and size-independent for E close to E_c .

To compute the level statistics of states around the WNs, we diagonalize the Hamiltonian (3) by imposing periodic boundary conditions in all directions in order to eliminate the edge state effects. Near the WNs, the DOSs decrease with $|E|$ algebraically such that a proper renormalization is needed to correctly compute $P(s)$. We also eliminate the systematic error in the histogram plots to increase the accuracy of $P(s)$ [41].

Results of IPR.—Figure 1(a) displays $\ln p_2(E = 0)$ v.s. $\ln L$ at $W = 4 < W_{c,1}$. The curve is a straight line with a slope (fractal dimension) of $D = 2.18 \pm 0.05$, in contrast to a normal extended state that occupies the whole space. Wavefunctions at WNs have a universal fractal structure in the sense that D does not depend on the disorder strength $W < W_{c,1}$. This is clearly shown by the D – W curve in Fig. 1(b). It is evident that $D \simeq 2.18$ is constant for $W < W_{c,1}$. However, for $W_{c,3} > W > W_{c,2}$, we find $D \simeq 3$ that indicates the state of $E = 0$ becomes a normal extended state, and the system becomes a DM. Above $W_{c,3}$, the zero energy state is localized with $D \simeq 0$, see the inset of Fig. 1(b). Our calculations of D are consistent with the direct WSM-to-DM transition.

To confirm the criticality of WNs, we perform the chi-square fit of $p_2(E)$ to Eq. (6) and plot $Y_L(E)$ for $W = 4$ in Fig. 1(c). If only systems of small sizes are considered, say $L \leq 18$, $Y_L(E)$ always increases with L , and one would conclude that all states are extended. However, we find $dY_L/dL = 0$ at WNs for $L > 18$ within numerical errors, instead of $dY_L/dL > 0$ for an extended state. The merging of $Y_L(E = 0)$

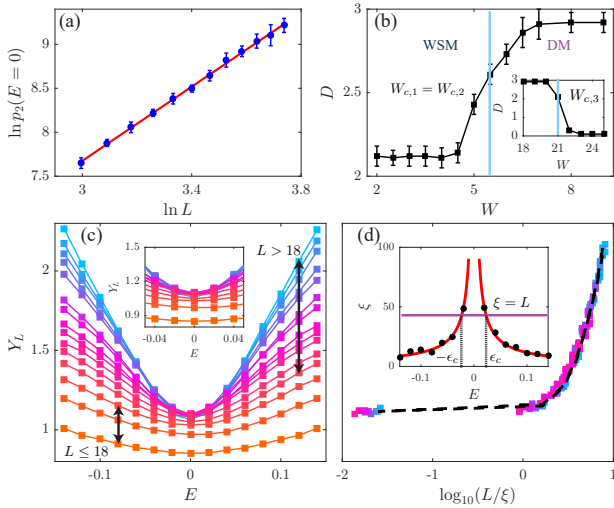


FIG. 1: (a) $\ln p_2(E=0)$ v.s. $\ln L$ for $W = 4$. The solid line is the linear fit of slope $D = 2.18 \pm 0.05$. (b) D v.s. W for $2 \leq W \leq 9$ and $18 \leq W \leq 24$ (Inset). (c) Y_L v.s. E for $L = 42, 40, 38, \dots, 14$ (from up to down) for $W = 4$. (d) Scaling function $f(x = \log_{10}(L/\xi))$. Black dash line connects points to guide eyes. Inset: $\xi(E, W = 4)$ v.s. E . Red solid line is the fit of $\xi = \xi_0|E|^{-\nu}$. Dash lines locate $-\epsilon_c(L)$ and $\epsilon_c(L)$. Error bars for all the data points are smaller than symbol sizes in (c) and (d).

indicates $E = 0$ is a critical point and a novel phase transition between an isolated critical state at WNs and extended states at $E \neq 0$, very similar to the phase transition from an isolated critical level to localized states in IQH systems [32].

Our data fit well to the one-parameter scaling hypothesis of $Y_L(E) = f(L/\xi)$ with $\xi = \xi_0|E|^{-\nu}$ for states near $E = 0$. From the chi-square fit of $p_2(E)$ for $L > 18$, we obtain $\nu = 0.89 \pm 0.05$, $y = 0.4 \pm 0.1$, $\xi_0 = 1.5 \pm 0.3$, and $C_3 = 3.2 \pm 0.1$ [40]. The goodness-of-fit $Q = 0.3$ is a quite satisfactory number, thus it supports $E = 0$ as a quantum critical point separating a critical state from extended states. The smooth scaling function $f(x = \log_{10}(L/\xi))$ with $\xi = \xi_0|E|^{-\nu}$ is shown in Fig. 1(d) obtained by collapsing all $Y_L(E)$ curves of different L into a single curve.

Results of $P(s)$.—Because $E = 0$ is an isolated critical point for $W < W_{c,1}$, one should expect that all states for a system of size L within a small energy range of $|E| < \epsilon_c$ indicated by the vertical dash lines in the inset of Fig. 1(d), where the critical energy is defined as $\epsilon_c = (\xi_0/L)^{1/\nu}$, look like fractals of dimension $D = 2.18$. The level spacing distribution $P(s)$ within the energy window is expected to follow the critical level statistics of Eq. (1) coming from the assumption of power-law decay of wavefunctions [33, 35, 36, 38]. Our conjecture is confirmed by Fig. 2(a). Apparently, $P(s) = P_c(s)$ only for states near WNs ($|E| < \epsilon_c = (\xi_0(W=4)/L)^{1/\nu} = 0.035$), while far away from the WNs (say $|E| \in [0.10, 0.11]$), $P(s) = P_{\beta=2}(s)$. We note also that $P(s)$ evolves from $P_{\beta=2}(s)$ to $P_c(s)$ as the energy window approached $[-\epsilon_c, \epsilon_c]$. Thus, although $P_c(s)$ persists at $|E| < \epsilon_c$ for finite L , it will happen only at WNs in the thermodynamics limit $L \rightarrow \infty$. Similar features have been observed by a fixed energy window and varying L (ϵ_c) [40].

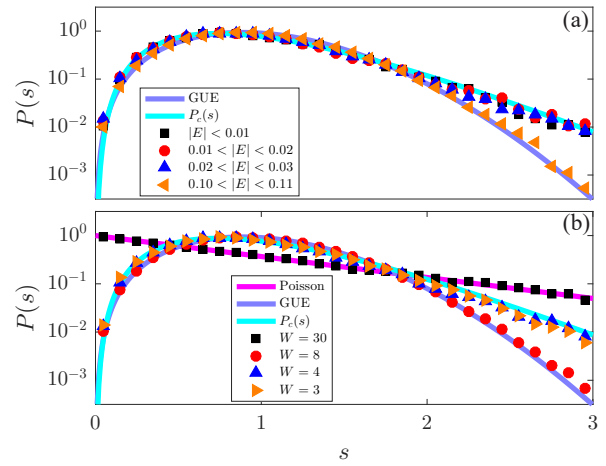


FIG. 2: (a) $P(s)$ for different energy windows at $W = 4$. The cyan and slate-blue lines are Eq. (1) and $P_{\beta=2}(s)$, respectively. (b) $P(s)$ for $W = 3, 4, 8, 30$ in a fixed energy window $E/t \in [-0.03, 0.03]$: For $W = 3, 4 < W_{c,1}$, numerical data of $P(s)$ agrees with $P_c(s)$. For $W_{c,3} > W = 8 > W_{c,2}$, $P(s)$ data falls on $P_{\beta=2}(s)$. For $W = 30 > W_{c,3}$, $P(s)$ accords with $P_{\text{Loc}}(s)$. Here $L = 30$.

We investigate now how $P(s)$ within energy range of $[-0.03, 0.03]$ changes with randomness strength W from the universal level distribution $P_c(s)$ at a weak disorder, where zero energy wavefunction is a fractal, to the Poisson distribution at extremely strong disorder, where the zero energy wavefunction is localized. Some representative results are shown in Fig. 2(b). At an extremely strong disorder $W = 30 > W_{c,3}$ where all states are localized, $P(s)$ (black squares) follows the Poisson statistics P_{Loc} (magenta line). While for $W_{c,3} > W = 8 > W_{c,2}$ such that the system is in the DM phase, $P(s)$ (red circles) follows the Wigner surmises $P_{\beta=2}(s)$. When the systems are WSMs, say $W = 4, 3 < W_{c,1}$, $P(s)$ are described by $P_c(s)$.

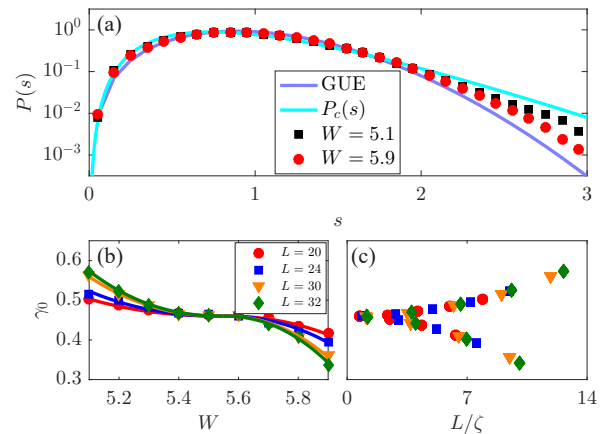


FIG. 3: (a) $P(s)$ for $W = 5.1$ and 5.9 at $L = 30$ and $|E| < 0.03$. Cyan and slate-blue lines are the same as those in Fig. 2. (b) γ_0 v.s. W for $L = 20, 24, 30, 32$. (c) Scaling function $g(x)$ of $\gamma_0(W, L)$.

Let us use above results to address the issue whether there

is a direct WSM-to-DM transition in the regime of $W_{c,1} < W < W_{c,2}$. If there is a topological insulator phase between disordered WSM and DM phases [21], one should expect $P(s)$ passing through the Poisson distribution on its way from $P_c(s)$ to $P_{\beta=2}(s)$. Figure 3(a) are two examples that show clearly $P(s)$ changing from $P_c(s)$ to $P_{\beta=2}(s)$ in the regime of $W_{c,1} < W < W_{c,2}$ without any sign of Poisson distribution. To further substantiate the assertion, we evaluate $\gamma_0(W, L)$ and show the results in Fig. 3(b). The transitions between the new universal level statistics ($\gamma_0 = 0.62$) and the Wigner-Dyson distribution ($\gamma_0 = 0$) become sharper for larger L . Besides, $\gamma_0(W, L)$ curves for different L cross at a single disorder $W = W_c \simeq 5.5$, indicate a quantum phase transition. We thus identify W_c as the transition point that is substantiated by the nice collapse of all data in the vicinity of W_c into a single parameter scaling function of

$$\gamma_0(W, L) = g(L/\zeta) \quad (7)$$

with the correlation length diverging as $\zeta = \zeta_0|W - W_c|^{-\nu}$, as shown in Fig. 3(c). Obviously, two different branches for $W < W_c$ and $W > W_c$ correspond to two distinct phases. We thus consider Fig. 3 as an empirical verification of the existence of WSM-to-DM quantum phase transitions such that states of $W < W_c$ ($W > W_c$) belong to the WSMs (the DMs) for $L \rightarrow \infty$.

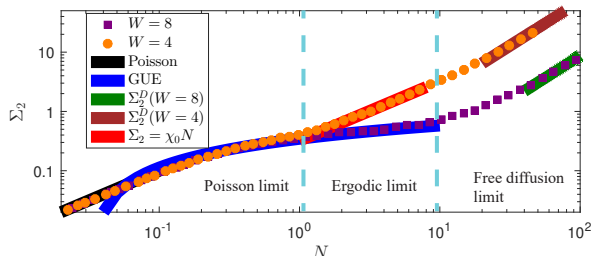


FIG. 4: Σ_2 v.s. N for $W = 4$ (orange circles) and 8 (purple squares). Here $L = 30$.

Results of $\Sigma_2(\Delta E)$.—We also compute the number variance $\Sigma_2(\Delta E)$ for various energy ranges $[-\Delta E/2, \Delta E/2]$ (around WNs) and disorders. Figure 4 displays $\Sigma_2(\Delta E)$ vs N for WSM ($W = 4$) and DM ($W = 8$). According to the orthodox theory [33, 38, 44], there exist two important energy scales: the Thouless energy E_T related to the dimensionless conductance of a mesoscopic system and the mean level spacing δ . By using the Kwant code, we numerically obtain $E_T/\delta = 11.1 \pm 0.5$ and 8.8 ± 0.4 for $W = 4$ and 8, respectively [45]. There are three interesting regions. One is the so-called free diffusion limit: $N = \Delta E/\delta \gg E_T/\delta$ where Σ_2 is given by $\Sigma_2^D = (\sqrt{2}/(12\pi^3))(\delta/E_T)^{3/2}N^{3/2}$ [44], see the violet ($W = 4$) and green ($W = 8$) lines without any fitting parameter. Our numerical data agree well with the theory. In another limit of $\Delta E \ll \delta$, $\Sigma_2(\Delta E)$ follow the Poisson behavior $\Sigma_2(\Delta E) = N$ because the level repulsion will not play any role when the probability of having two levels in ΔE is negligible. Our numerical data for both WSM and DM agree again with this

expectation, evident by the fact that black line of $\Sigma_2(\Delta E) = N$ passes through all data points for $N < 0.1$. Thus, the level statistics of WSMs and DMs are the same in the two regions.

The intermediate region is the so-called ergodic limit of $\delta < \Delta E < E_T$, where the level statistics of WSMs and DMs are completely different. For DMs, the level repulsion dominates the statistics, leading to the Wigner-Dyson statistics, $\Sigma_2 = (\ln(2\pi N) + 1 + e^\gamma)/\pi^2$ (blue curve), where $\gamma \simeq 0.577$ is the Euler's constant [28]. Indeed, our data for $W = 8$ agree with this prediction very well for $0.5 < N < 10$. Remarkably, a deviation from the Wigner-Dyson statistics is obviously seen for $W = 4$, since the overlap of wavefunctions near WNs are much less than the normal extended states. The collective organization of wavefunctions near WNs is much weaker, and Σ_2 shows a linear behaviour in our data with a universal slope $\chi = 0.2 \pm 0.1$ (red line) [46].

Remarks.—(1) A natural question is whether the physics and critical exponents such as $\gamma_0 = 0.62$ and $\nu = 0.89$ are model-independent [47]. As shown in the Supplemental Materials [40], the answer is yes, at least within the models used. Furthermore, γ_0 and ν independently obtained satisfy well the relationship of $\gamma_0 = 1 - 1/(\nu d)$ from the theory [33, 38]. (2) The anomalous dimension $\Delta_2 = D - d = -0.82$ agrees well with an analytical result [48]. (3) The estimated $\nu = 0.89$ is consistent with result of the finite-size scaling of DOSs [15, 18] on double-WN models, but smaller than those by renormalization group calculations on single-WN models [49]. (4) The spectral compressibility χ is related to the fractal dimension D by $\chi = (d - D)/(2d)$ [38]. Numerical values of $\chi = 0.2$ and $D = 2.18$ agree with this relationship within numerical errors. (5) Cold atom system supporting WNs [51, 52] is the ideal platform to verify our theoretical prediction of the novel level statistics [53].

In conclusion, the WNs ($E = 0$) in weakly disordered WSMs are an isolated critical point in the sense that the zero energy wavefunction is a fractal of dimension 2.18. There exists a correlation length diverging as $\xi = \xi_0|E|^{-\nu}$ with $\nu = 0.89$ near the WNs. Wavefunctions exhibit fractal structures at the length scale smaller than ξ , and homogeneous structures at the length scale larger than ξ . Near the WNs and in a narrow energy window smaller than $[-\epsilon_c, \epsilon_c]$ ($\epsilon_c = (\xi_0/L)^{-\nu}$), the nearest-neighbor level spacing distribution is well described by the critical level statistics of $P_c(s) = C_1 s^2 \exp[-C_2 s^{2-\gamma_0}]$ with $\gamma_0 = 0.62 \pm 0.07$, in contrast to the Wigner-Dyson distribution far from the WNs. Similar conclusion is obtained for the level number variance $\Sigma_2(\Delta E) = \chi N$ around the WNs with a universal spectral compressibility $\chi = 0.2 \pm 0.1$. The fractal nature and the level statistics of WNs thus provide authentic fingerprints of disordered WSMs.

C.W. would like to thank Ying Su for valuable discussions of the phase diagram of disordered WSMs. This work is supported by the National Natural Science Foundation of China (Grants No. 11374249 and 11704061) and Hong Kong RGC (Grants No. 16301518 and 16300117). C.W. is supported by UESTC and the China Postdoctoral Science Foundation (Grants No. 2017M610595 and 2017T100684). P.Y.

is supported by the National Natural Science Foundation of China under Grant No. 11604041 and the National Thousand-Young-Talent Program of China.

* Corresponding author: phxwan@ust.hk

- [1] X. Wan, A. M. Turner, A. Vishwanath, and S. Y. Savrasov, Topological semimetal and Fermi-arc surface states in the electronic structure of pyrochlore iridates, *Phys. Rev. B* **83**, 205101 (2011).
- [2] K.-Y. Yang, Y.-M. Lu, and Y. Ran, Quantum Hall effects in a Weyl semimetal: Possible application in pyrochlore iridates, *Phys. Rev. B* **84**, 075129 (2011).
- [3] A. A. Burkov and L. Balents, Weyl Semimetal in a Topological Insulator Multilayer, *Phys. Rev. Lett.* **107**, 127205 (2011).
- [4] H. Weng, C. Fang, Z. Fang, B. A. Bernevig, and X. Dai, Weyl Semimetal Phase in Noncentrosymmetric Transition-Metal Monophosphides, *Phys. Rev. X* **5**, 011029 (2015).
- [5] S. Y. Xu, I. Belopolski, N. Alidoust, M. Neupane, G. Bian, C. L. Zhang, R. Sankar, G. Chang, Z. Yuan, C. C. Lee, S. M. Huang, H. Zheng, J. Ma, D. S. Sanchez, B. K. Wang, A. Bansil, F. Chou, P. P. Shibaev, H. Lin, S. Jia, and M. Z. Hasan, Discovery of a Weyl fermion semimetal and topological Fermi arcs, *Science* **349**, 613 (2015).
- [6] L. Lu, Z. Wang, D. Ye, L. Ran, L. Fu, J. D. Joannopoulos, M. Soljačić, Experimental observation of Weyl points, *Science* **349**, 622 (2015).
- [7] C. Shekhar, A. K. Nayak, Y. Sun, M. Schmidt, M. Nicklas, I. Leermakers, U. Zeitler, Y. Skourski, J. Wosnitza, Z. Liu, Y. Chen, W. Schnelle, H. Borrmann, Y. Grin, C. Felser, and B. Yan, Extremely large magnetoresistance and ultrahigh mobility in the topological Weyl semimetal candidate NbP, *Nat. Phys.* **11**, 645 (2015).
- [8] A. Burkov, Chiral anomaly without relativity, *Science* **350**, 378 (2015).
- [9] B. Sbierski, G. Pohl, E. J. Bergholtz, and P. W. Brouwer, Quantum Transport of Disordered Weyl Semimetals at the Nodal Point, *Phys. Rev. Lett.* **113**, 026602 (2014).
- [10] S. V. Syzranov, L. Radzihovsky, and V. Gurarie, Critical Transport in Weakly Disordered Semiconductors and Semimetals, *Phys. Rev. Lett.* **114**, 166601 (2015).
- [11] J. H. Pixley, P. Goswami, and S. Das Sarma, Anderson Localization and the Quantum Phase Diagram of Three Dimensional Disordered Dirac Semimetals, *Phys. Rev. Lett.* **115**, 076601 (2015).
- [12] B. Roy, R.-J. Slager, and V. Jurii, Global Phase Diagram of a Dirty Weyl Liquid and Emergent Superuniversality, *Phys. Rev. X* **8**, 031076 (2018).
- [13] S. Bera, J. D. Sau, and B. Roy, Dirty Weyl semimetals: Stability, phase transition, and quantum criticality, *Phys. Rev. B* **93**, 201302(R) (2016).
- [14] P. Goswami, and S. Chakravarty, Quantum criticality between topological and band insulators in 3+1 dimensions, *Phys. Rev. Lett.* **107**, 196803 (2011).
- [15] K. Kobayashi, T. Ohtsuki, K. T. Imura, and I. F. Herbut, Density of states scaling at the semimetal to metal transition in three dimensional topological insulators, *Phys. Rev. Lett.* **112**, 016402 (2014).
- [16] C.-Z. Chen, J. Song, H. Jiang, Q. Sun, Z. Wang, and X. C. Xie, Disorder and Metal-Insulator Transitions in Weyl Semimetals, *Phys. Rev. Lett.* **115**, 246603 (2015).
- [17] H. Shapourian and T. L. Hughes, Phase diagrams of disordered Weyl semimetals *Phys. Rev. B* **93**, 075108 (2016).
- [18] S. Liu, T. Ohtsuki, and R. Shindou, Effect of disorder in a three-dimensional layered Chern insulator, *Phys. Rev. Lett.* **116**, 066401 (2016).
- [19] R. Nandkishore, D. A. Huse, and S. L. Sondhi, Rare region effects dominate weakly disordered three-dimensional Dirac points, *Phys. Rev. B* **89**, 245110 (2014).
- [20] J. H. Pixley, D. A. Huse, and S. Das Sarma, Rare-Region-Induced Avoided Quantum Criticality in Disordered Three-Dimensional Dirac and Weyl Semimetals, *Phys. Rev. X* **6**, 021042 (2016).
- [21] Y. Su, X. S. Wang, and X. R. Wang, A generic phase between disordered Weyl semimetal and diffusive metal, *Sci. Rep.* **7**, 14382 (2017).
- [22] K. Ziegler and A. Sinner, Short Note on the Density of States in 3D Weyl Semimetals, *Phys. Rev. Lett.* **121**, 166401 (2018).
- [23] E. P. Wigner, Characteristic Vectors of Bordered Matrices With Infinite Dimensions, *Annals of Mathematics* **62**, 548 (1955).
- [24] O. Bohigas, M. J. Giannoni, and C. Schmit, Characterization of Chaotic Quantum Spectra and Universality of Level Fluctuation Laws, *Phys. Rev. Lett.* **52**, 1 (1984).
- [25] J. J. M. Verbaarschot and T. Wettig, Random Matrix Theory and Chiral Symmetry in QCD, *Annu. Rev. Nucl. Part. Sci.* **50**, 343 (2000).
- [26] D. Sánchez and M. Büttiker, Magnetic-Field Asymmetry of Nonlinear Mesoscopic Transport, *Phys. Rev. Lett.* **93**, 106802 (2004).
- [27] F. Franchini and V. E. Kravtsov, Horizon in Random Matrix Theory, the Hawking Radiation, and Flow of Cold Atoms, *Phys. Rev. Lett.* **103**, 166401 (2009).
- [28] M. L. Mehta, *Random matrices* (Elsevier, 2004).
- [29] $\beta = 1$ for systems with time-reversal symmetry and spin-rotation symmetry is called the Gaussian orthogonal ensemble; $\beta = 2$ for systems without time-reversal symmetry is called the Gaussian unitary ensemble; $\beta = 4$ for systems with time-reversal symmetry and no spin-rotation symmetry is called the Gaussian symplectic ensemble.
- [30] The predicted vanishing DOSs at WNs have also attracted many numerical studies [11, 13, 15, 18–20, 22]. Most of those agreed with the zero DOS at WNs, but some recent works [20, 22] concluded that it cannot exist at nonzero disorder due to rare region effects, and no WSM phase is allowed at an arbitrary weak disorder if zero DOS at WNs is demanded.
- [31] G. Xiong, S.-D. Wang, Q. Niu, D.-C. Tian, and X. R. Wang, Metallic Phase in Quantum Hall Systems due to Inter-Landau-Band Mixing, *Phys. Rev. Lett.* **87**, 216802 (2001).
- [32] C. Wang, Y. Avishai, Y. Meir, and X. R. Wang, Anti-levitation in integer quantum Hall systems, *Phys. Rev. B* **89**, 045314 (2014).
- [33] B. L. Altshuler and B. I. Shklovskii, Repulsion of energy levels and conductivity of small metal samples, *Sov. Phys. JETP* **64**, 127 (1986).
- [34] B. I. Shklovskii, B. Shapiro, B. R. Sears, P. Lambrianides, and H. B. Shore, Statistics of spectra of disordered systems near the metal-insulator transition, *Phys. Rev. B* **47**, 11487 (1993).
- [35] V. E. Kravtsov, I. V. Lerner, B. L. Altshuler, and A. G. Aronov, Universal spectral correlations at the mobility edge, *Phys. Rev. Lett.* **72**, 888 (1994).
- [36] A. G. Aronov, V. E. Kravtsov, and I. V. Lerner, Spectral Correlations in Disordered Electronic Systems: Crossover from Metal to Insulator Regime, *Phys. Rev. Lett.* **74**, 1174 (1995).
- [37] R. Klesse and M. Metzler, Spectral Compressibility at the Metal-Insulator Transition of the Quantum Hall Effect, *Phys.*

- Rev. Lett. **79**, 721 (1997).
- [38] A. D. Mirlin, Statistics of energy levels and eigenfunctions in disordered systems, Phys. Rep. **326**, 259 (2000).
- [39] A. M. Garcia-Garca, Semiclassical Theory of the Anderson Transition, Phys. Rev. Lett. **100**, 076404 (2008).
- [40] See Supplemental Materials at <http://link.aps.org/supplemental>.
- [41] C. Wang and X. R. Wang, Anderson transition of two-dimensional spinful electrons in the Gaussian unitary ensemble, Phys. Rev. B **96**, 104204 (2017).
- [42] X. R. Wang, Y. Shapir, and M. Rubinstein, Analysis of multiscaling structure in diffusion-limited aggregation: A kinetic renormalization-group approach, Phys. Rev. A **39**, 5974 (1989).
- [43] M. Janssen, Phys. Rep. **295**, 1 (1998).
- [44] E. Akkermans, and G. Montambaux, Mesoscopic physics of electrons and photons (Cambridge university press, 2007).
- [45] C. W. Groth, M. Wimmer, A. R. Akhmerov, and X. Waintal, Kwant: a software package for quantum transport, New J. Phys. **16**, 063065 (2014).
- [46] We find that χ is independent of disorder strengths W and system sizes L . See the Supplemental Materials for more details.
- [47] To support the universality of the level statistics around WNs, we perform the same calculations on a different lattice models of disordered WSM reported in Ref. [18] and find that γ_0 and ν are model-independent and disorder-independent. See the Supplemental Materials [40] for more details.
- [48] S. V. Syzranov, V. Gurarie, L. Radzihovsky, Multifractality at non-Anderson disorder-driven transitions in Weyl semimetals and other systems, Ann. Phys. **373**, 694 (2016).
- [49] We obtain $\nu = 0.89 \pm 0.05$. The value is smaller than those from renormalization group calculations, e.g., $\nu = 1$ for one-loop [14], $\nu = 1.14$ for two-loops [12], and $\nu = 1.47 \pm 0.03$ from numerical data [50]. Note that those calculations were based on the single-WN model in the $2 + \epsilon$ dimension. In reality, WNs must appear in pairs. The white-noisy disorders will surely couple different WNs together [21]. Thus, the applicability of the renormalization group approach to finding critical exponent ν are questionable for the spatial uncorrelated disorders considered here.
- [50] B. Sbierski, E. J. Bergholtz, and P. W. Brouwer, Quantum critical exponents for a disordered three-dimensional Weyl node, Phys. Rev. B **92**, 115145 (2015).
- [51] T. Dubek, C. J. Kennedy, L. Lu, W. Ketterle, M. Soljai, and H. Buljan, Weyl Points in Three-Dimensional Optical Lattices: Synthetic Magnetic Monopoles in Momentum Space, Phys. Rev. Lett. **114**, 225301 (2015).
- [52] X. Li and S. D. Sarma, Exotic topological density waves in cold atomic Rydberg-dressed fermions, Nat. Commun. **6**, 7137 (2015).
- [53] S.-L. Zhu, B. Wang, and L.-M. Duan, Simulation and Detection of Dirac Fermions with Cold Atoms in an Optical Lattice, Phys. Rev. Lett. **98**, 260402 (2007).